Intersymbol and Intercarrier Interference in OFDM Transmissions Through Highly Dispersive Channels

Wallace Alves Martins
Université du Luxembourg, Luxembourg
Universidade Federal do Rio de Janeiro, Brazil
wallace.alvesmartins@uni.lu

Fernando Cruz–Roldán
Universidad de Alcalá
Alcalá de Henares (Madrid), Spain
fernando.cruz@uah.es

Marc Moonen
Katholieke Universiteit Leuven
Leuven, Belgium
Marc.Moonen@esat.kuleuven.be

Paulo Sergio Ramirez Diniz
Universidade Federal do Rio de Janeiro
Rio de Janeiro, Brazil
diniz@smt.ufrj.br

***Abstract*—This work quantifies intersymbol and intercarrier interference induced by very dispersive channels in OFDM systems. The resulting achievable data rate for suboptimal OFDM transmissions is derived based on the computation of the actual signal-to-interference-plus-noise ratio for arbitrary length finite duration channel impulse responses. Simulation results point to significant differences between data rates obtained via conventional formulations, for which interference is supposed to be limited to two or three blocks, versus the data rates considering the actual channel dispersion.**

***Index Terms*—Orthogonal frequency-division multiplexing, highly dispersive channels, intersymbol interference, intercarrier interference, cyclic prefix, zero padding**

I. Introduction

Since its origins in the analog [1] and digital [2] domains, the orthogonal frequency-division multiplexing (OFDM) system has striven to combat interference induced by frequency-selective channels [3]. A major breakthrough was the use of redundant elements, such as cyclic prefix, for preserving orthogonality among subcarriers at the receiver [4].

Practical wireless broadband communications use increasingly high sampling rates while trying to meet the demands for high data rates. In this context, the redundancy overhead turns out to be a big issue due to spectral-efficiency losses. Furthermore, as some practical wired applications (e.g., digital subscriber lines, including ADSL, VDSL, and more recently, G.Fast) work with highly dispersive channels, it can be virtually impossible to append so many redundant elements in the transmission, calling for alternative solutions, such as prefiltering at the receiver side to shorten the effective channel model [5]. Besides, the use of on-channel repeaters to extend system coverage [6] can induce delays which are longer than those the guard interval was originally designed to cope with.

The aforementioned issues motivated many works to analyze ISI/ICI in OFDM systems with insufficient redundancy [7]–[23]. Perhaps, the first attempt to analyze systematically the harmful ISI/ICI effects are the works in [7], [8], [24] in which preliminary results in terms of interference spectral power are presented. The authors in [9] analyze ISI interference in OFDM-based high-definition television (HDTV). The works in [10] address time-variant channels that induce Doppler effects. A landmark work is [11], which presents the interference power due to the tails of the channel impulse response (CIR). The works [12], [13] use the ISI/ICI interference analyses to design the front-end prefilter employed at the receiver side for channel shortening in xDSL applications. The work in [14] uses the results from [11] to show it might be useful to allow the existence of ISI/ICI due to insufficient guard periods, as long as the transceiver is aware of it—via feedback mechanism of channel-state information (CSI). The authors in [19] analyze the ISI/ICI impacts on a power-line communication (PLC) system, whereas [20] optimize the redundancy length for a PLC system, allowing for the existence of controlled ISI/ICI. A similar kind of optimization is also conducted for coherent optical communications in [21]. The works [22] analyze the ISI/ICI effects from a theoretical and an experimental viewpoints for wireless local area networks. The works [25]–[28] address the design/analysis of more general transceivers or equalizers, mostly for doubly-selective channel models.

All of these works start from a common point—the analysis of ISI/ICI for a general setup where the amount of redundant elements can be smaller than the delay spread of the channel—to eventually achieve different goals. We shall start from the same point, but *without imposing any kind of constraints upon the order of the CIR*, which is only assumed to have finite duration. This eventually implies that the proposed analysis can be applied to the cases where the interference is due to several data blocks, not being limited to two or three blocks, as all previous works do. As mentioned before, this is especially important in delay-constrained applications working in highly dispersive environments where the number of subcarriers cannot be set larger than the order of the CIR. Besides, the proposed analysis unifies and generalizes many

This study was financed in part by Capes, CNPq, and Faperj, Brazilian research councils. The work was also partially supported by the Spanish Ministry of Economy and Competitiveness through project TEC2015-64835-C3-1-R and by the Spanish Ministry of Education, Culture and Sports through Research Grant PRX17/0080.

978-9-0827-9703-9/19/$31.00 ©2019 IEEE

Authorized licensed use limited to: KU Leuven Libraries. Downloaded on December 17,2020 at 09:02:11 UTC from IEEE Xplore. Restrictions apply.

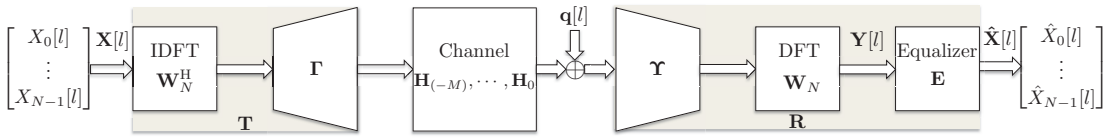


Fig. 1. Block diagram of an OFDM transceiver.

of the aforementioned works, providing closed-form matrix expressions as functions of the channel taps that are easy to use for different purposes—including the ones listed above. Both cyclic-prefix and zero-padding OFDM transmissions are considered and a fine distinction between two types of ICI is provided. As for the application of the proposed analysis, this work focuses on providing *achievable data rates for suboptimal OFDM transmissions* based on the computation of signal-to-interference-plus-noise ratios (SINRs) for arbitrary length finite duration CIR.

II. System Model

Let us consider an OFDM transceiver model as depicted in Fig. 1. The data samples $X_k[l]$, with $k \in \mathcal{N} \triangleq \{0, 1, \cdots, N-1\} \subset \mathbb{N}$, belong to a particular constellation $\mathcal{C} \subset \mathbb{C}$, such as QAM or PSK, and comprise vector $\mathbf{X}[l]$ at the (block) time index $l \in \mathbb{Z}$. After the transmission/reception process, the reconstructed data samples are denoted as $\hat{X}_k[l]$, with $k \in \mathcal{N}$, and comprise the reconstructed data vector $\hat{\mathbf{X}}[l]$.

The cyclic-prefix OFDM (CP-OFDM) is described by the following transmitter and receiver matrices, respectively:

$$\mathbf{T}_{\mathrm{CP}} \triangleq \underbrace{\begin{bmatrix} \mathbf{0}_{\mu\times(N-\mu)} & \mathbf{I}_\mu \\ & \mathbf{I}_N \end{bmatrix}}_{\mathbf{\Gamma}_{\mathrm{CP}} \in \mathbb{C}^{N_0 \times N}} \cdot \mathbf{W}_N^{\mathrm{H}}, \tag{1}$$

$$\mathbf{R}_{\mathrm{CP}} \triangleq \mathbf{E} \cdot \mathbf{W}_N \cdot \underbrace{\begin{bmatrix} \mathbf{0}_{N\times\mu} & \mathbf{I}_N \end{bmatrix}}_{\mathbf{\Upsilon}_{\mathrm{CP}} \in \mathbb{C}^{N \times N_0}}, \tag{2}$$

where $N_0 \triangleq N + \mu \in \mathbb{N}$ denotes the size of the transmitted data vector after appending $\mu < N$ redundant elements,[1] $\mathbf{W}_N$ is the normalized $N \times N$ discrete Fourier transform (DFT) matrix with entries $[\mathbf{W}_N]_{kn} = \mathrm{e}^{-\mathrm{j}\frac{2\pi}{N}kn}/\sqrt{N}$, $\mathbf{I}_N$ is the $N \times N$ identity matrix, $\mathbf{0}_{N\times\mu}$ is an $N \times \mu$ matrix whose entries are zero, and $\mathbf{E} \in \mathbb{C}^{N\times N}$ is an equalizer diagonal matrix.

An alternative OFDM system inserts zeros as redundancy and is called zero-padding OFDM (ZP-OFDM). There are many variants of ZP-OFDM. A common choice is the ZP-OFDM-OLA (overlap-and-add), with:

$$\mathbf{T}_{\mathrm{ZP}} \triangleq \underbrace{\begin{bmatrix} \mathbf{I}_N \\ \mathbf{0}_{\mu\times N} \end{bmatrix}}_{\mathbf{\Gamma}_{\mathrm{ZP}} \in \mathbb{C}^{N_0 \times N}} \cdot \mathbf{W}_N^{\mathrm{H}}, \tag{3}$$

$$\mathbf{R}_{\mathrm{ZP}} \triangleq \mathbf{E} \cdot \mathbf{W}_N \cdot \underbrace{\begin{bmatrix} \mathbf{I}_N & \\ & \mathbf{0}_{(N-\mu)\times\mu} \end{bmatrix}}_{\mathbf{\Upsilon}_{\mathrm{ZP}} \in \mathbb{C}^{N \times N_0}}. \tag{4}$$

[1] In principle, there is no point in using $\mu \geq N$ in practice.

The channel model is represented by a causal finite duration impulse response (FIR) filter with coefficients $h_0, \ldots, h_\nu \in \mathbb{C}$ of order $\nu \in \mathbb{N}$, and an additive noise vector $\mathbf{q}[l] \in \mathbb{C}^{N_0}$. In fact, the FIR model can also be regarded as an overall channel impulse response, encompassing any pulse shaping and front-end receive prefiltering. Thus, assuming a synchronization delay $\Delta \in \{0, 1, \ldots, N_0 - 1\}$,[2] the number of data vectors that may affect the reception of a single data vector is $M+2$, where

$$M \triangleq \left\lceil \frac{\nu}{N_0} \right\rceil, \tag{5}$$

in which $\lceil \cdot \rceil$ stands for the ceiling function. Hence, the reconstructed data vector can be written as

$$\hat{\mathbf{X}}[l] = \sum_{m=-1}^{M} \mathbf{R} \cdot \mathbf{H}_{(-m)} \cdot \mathbf{T} \cdot \mathbf{X}[l-m] + \mathbf{R} \cdot \mathbf{q}[l], \tag{6}$$

where $\mathbf{H}_{(-m)}$ is an $N_0 \times N_0$ matrix, in which, for $0 \leq b, c \leq N_0 - 1$, one has

$$\left[\mathbf{H}_{(-m)}\right]_{b,c} \triangleq \begin{cases} 0, & mN_0 + b - c + \Delta < 0, \\ h_{mN_0+b-c+\Delta}, & 0 \leq mN_0 + b - c + \Delta \leq \nu, \\ 0, & mN_0 + b - c + \Delta > \nu. \end{cases} \tag{7}$$

Note that in (6), up to $M+2$ data vectors may contribute to the reconstructed vector $\hat{\mathbf{X}}[l]$. In fact, this number can be smaller, depending on the delay Δ. Indeed, based on (5), one can write $\nu = (M-1)N_0 + \rho + 1$, with ρ being a number in the set $\{0, 1, \ldots, N_0 - 1\}$. Based on (7), if there is perfect synchronization (i.e., $\Delta = 0$), then $\mathbf{H}_{(1)} = \mathbf{0}_{N_0\times N_0}$ and the reconstructed data vector is affected by at most $M+1$ transmitted data vectors. In this case, the last matrix $\mathbf{H}_{(-M)}$ has only $\rho + 1$ nonzero rows. This eventually implies that, for $\Delta > \rho$, what would be the $(M+2)^{\mathrm{th}}$ channel matrix will actually be a null matrix, and again up to $M+1$ vectors affect $\hat{\mathbf{X}}[l]$. In summary, the number of data vectors contributing to the reconstructed vector is up to $M+2$ whenever Δ is chosen within the set $\{1, 2, \ldots, \rho\}$, or otherwise up to $M+1$.

Considering the scenarios in which the redundancy is long enough, i.e. $1 \leq \nu \leq \mu$, one has $M = 1$. In that case, the received data vector at time l might be affected only by the transmitted data vectors at times $l+1$, l, and $l-1$, for a nonzero delay Δ. As mentioned before, when $\Delta = 0$, one has $\mathbf{H}_{(1)} = \mathbf{0}_{N_0\times N_0}$, and matrices $\mathbf{\Upsilon}$ and $\mathbf{\Gamma}$ are able to eliminate the interference induced by the transmitted data vector at $l-1$, i.e., $\mathbf{\Upsilon} \cdot \mathbf{H}_{(-1)} \cdot \mathbf{\Gamma} = \mathbf{0}_{N\times N}$. In addition, one has that $\mathbf{\Upsilon} \cdot \mathbf{H}_0 \cdot \mathbf{\Gamma}$

[2] In fact, Δ could be any natural number, but we assume $\Delta \in \{0, 1, \ldots, N_0 - 1\}$ for the sake of simplicity.

Authorized licensed use limited to: KU Leuven Libraries. Downloaded on December 17,2020 at 09:02:11 UTC from IEEE Xplore. Restrictions apply.

is a right-circulant matrix of dimension $N \times N$ that can be diagonalized by the DFT matrix. As a result,

$$\hat{\mathbf{X}}[l] = \mathbf{E} \cdot \mathbf{D} \cdot \mathbf{X}[l] + \mathbf{R} \cdot \mathbf{q}[l], \tag{8}$$

where the diagonal matrix $\mathbf{D}$ is

$$\mathbf{D} \triangleq \operatorname{diag}\left\{ \sqrt{N}\mathbf{W}_N \cdot \begin{bmatrix} \mathbf{h} \\ \mathbf{0}_{(N-\nu-1)\times 1} \end{bmatrix} \right\}, \tag{9}$$

in which $\mathbf{h} \triangleq [\, h_0 \;\; h_1 \;\; \cdots \;\; h_\nu \,]^{\mathrm{T}}$. As can be noted, there are no ISI or ICI when $\nu \leq \mu$.

The equalizer $\mathbf{E}$ for this transceiver can be defined in several ways, where the most popular ones are the zero-forcing (ZF) and the minimum mean-squared error (MMSE) equalizers, with $\mathbf{E}_{\mathrm{ZF}} \triangleq \mathbf{D}^{-1}$ or $\mathbf{E}_{\mathrm{MMSE}} \triangleq \mathbf{D}^{H} \cdot \left(\mathbf{D} \cdot \mathbf{D}^{H} + \frac{1}{\mathrm{SNR}}\mathbf{I}_N\right)^{-1}$, where SNR stands for signal-to-noise ratio. In the latter case, the transmitted symbols and environment noise are wide-sense stationary (WSS), mutually independent, white random sequences.

As mentioned before, some previous works have analyzed the case where $\nu > \mu$, but with the restriction of having $\nu \leq N_0$. Next section presents an analysis for general ν.

III. ISI/ICI Analysis

This section focuses on OFDM transceivers with insufficient number of redundant elements, i.e., $\nu > \mu$. In this case, the received data vector at time l can be affected by the transmitted data vectors at times $l+1, l, l-1, \ldots, l-M$, and matrices $\mathbf{\Upsilon}$ and $\mathbf{\Gamma}$ cannot eliminate all ISI/ICI.

One can rewrite eq. (6) as

$$\begin{aligned}\hat{\mathbf{X}}[l] = \sum_{\substack{m=-1 \\ m\neq 0}}^{M} \mathbf{E} \cdot \underbrace{\mathbf{W}_N \cdot \mathbf{\Upsilon} \cdot \mathbf{H}_{(-m)} \cdot \mathbf{\Gamma} \cdot \mathbf{W}_N^{\mathrm{H}}}_{\mathbf{A}_m^{\mathrm{ISI,ICI_2}}} \cdot \mathbf{X}[l-m] \\ + \mathbf{E} \cdot \underbrace{\mathbf{W}_N \cdot \mathbf{\Upsilon} \cdot \mathbf{H}_0 \cdot \mathbf{\Gamma} \cdot \mathbf{W}_N^{\mathrm{H}}}_{\mathbf{B}^{\mathrm{des,ICI_1}}} \cdot \mathbf{X}[l] + \mathbf{E} \cdot \underbrace{\mathbf{W}_N \cdot \mathbf{\Upsilon}}_{\mathbf{G}^{\mathrm{noise}}} \cdot \mathbf{q}[l].\end{aligned} \tag{10}$$

The desirable signal of (10) is

$$\hat{\mathbf{X}}_{\mathrm{des}}[l] = \mathbf{E} \cdot \mathbf{B}^{\mathrm{des}} \cdot \mathbf{X}[l], \tag{11}$$

in which $\mathbf{B}^{\mathrm{des}}$ is a diagonal matrix with elements

$$\left[\mathbf{B}^{\mathrm{des}}\right]_{i,i} \triangleq \left[\mathbf{B}^{\mathrm{des,ICI_1}}\right]_{i,i}. \tag{12}$$

The difference between (10) and (11) defines the ISI and ICI. Now, the products $\mathbf{\Upsilon} \cdot \mathbf{H}_{(-m)} \cdot \mathbf{\Gamma}$, cannot be expressed as $N \times N$ right-circulant matrices, and therefore they cannot be diagonalized using DFTs. Based on [24], the interference can be classified into three different types:

- ISI: This is the interference from the data vector transmitted at time $l-m$, with $m \in \{-1, 1, 2, \ldots, M\}$, in the considered data vector transmitted at time l on the same subcarrier. All diagonal elements $\left[\mathbf{A}_m^{\mathrm{ISI,ICI_2}}\right]_{i,i}$ contribute to this interference.
- Type-1 ICI ($\mathrm{ICI_1}$): This is the interference among different subcarriers belonging to the considered data vector transmitted at time l. It appears as a consequence of the elements $\left[\mathbf{B}^{\mathrm{ICI_1}}\right]_{i,j}$, $i \neq j$, where $\mathbf{B}^{\mathrm{ICI_1}} \triangleq \mathbf{B}^{\mathrm{des,ICI_1}} - \mathbf{B}^{\mathrm{des}}$. Note that $\left[\mathbf{B}^{\mathrm{ICI_1}}\right]_{i,i} = 0$.
- Type-2 ICI ($\mathrm{ICI_2}$): This is the interference among different subcarriers of the data vector transmitted at time $l-m$, with $m \in \{-1, 1, 2 \ldots, M\}$, in the considered data vector transmitted at time l. The elements $\left[\mathbf{A}_m^{\mathrm{ISI,ICI_2}}\right]_{i,j}$, $i \neq j$, contribute to this interference.

Finally, the contribution of noise $\mathbf{q}[l]$ to the reconstructed data vector $\hat{\mathbf{X}}[l]$ depends on matrix $\mathbf{G}^{\mathrm{noise}}$.

IV. SINR Analysis and Applications

This section presents an application of the previous ISI/ICI analysis for conducting an SINR analysis of OFDM systems, which can then be employed in many applications, including computing achievable data rates. We shall start with the signals before the multiplication by the equalizer matriz $\mathbf{E}$. Based on (10) and (11), one has

$$\begin{aligned}\mathbf{Y}[l] \triangleq \mathbf{B}^{\mathrm{des,ICI_1}} \cdot \mathbf{X}[l] + \sum_{\substack{m=-1 \\ m\neq 0}}^{M} \mathbf{A}_m^{\mathrm{ISI,ICI_2}} \cdot \mathbf{X}[l-m] \\ + \mathbf{G}^{\mathrm{noise}} \cdot \mathbf{q}[l],\end{aligned} \tag{13}$$

$$\mathbf{Y}_{\mathrm{des}}[l] \triangleq \mathbf{B}^{\mathrm{des}} \cdot \mathbf{X}[l]. \tag{14}$$

Now, assuming the transmitted symbols and the noise signal are WSS, mutually independent, white random sequences with zero means and variances σ_X^2 and σ_Q^2, respectively, then one can compute the covariance matrices of the desired signal ($\mathbf{C}_{\mathrm{s}}$), of the noise component ($\mathbf{C}_{\mathrm{n}}$), and of ISI/ICI ($\mathbf{C}_{\mathrm{i}}$). Indeed, one has

$$\mathbf{C}_{\mathrm{s}} = E\left\{\mathbf{Y}_{\mathrm{des}}[l] \cdot \mathbf{Y}_{\mathrm{des}}^{\mathrm{H}}[l]\right\} = \sigma_X^2 \cdot \mathbf{B}^{\mathrm{des}} \cdot (\mathbf{B}^{\mathrm{des}})^{\mathrm{H}}, \tag{15}$$

$$\begin{aligned}\mathbf{C}_{\mathrm{i}} + \mathbf{C}_{\mathrm{n}} &= E\left\{(\mathbf{Y}[l] - \mathbf{Y}_{\mathrm{des}}[l]) \cdot (\mathbf{Y}[l] - \mathbf{Y}_{\mathrm{des}}[l])^{\mathrm{H}}\right\} \\ &= \underbrace{\sigma_X^2 \left(\mathbf{B}^{\mathrm{ICI_1}} \cdot (\mathbf{B}^{\mathrm{ICI_1}})^{\mathrm{H}} + \sum_{\substack{m=-1 \\ m\neq 0}}^{M} \mathbf{A}_m^{\mathrm{ISI,ICI_2}} \cdot (\mathbf{A}_m^{\mathrm{ISI,ICI_2}})^{\mathrm{H}} \right)}_{\mathbf{C}_{\mathrm{i}}} \\ &\quad + \underbrace{\sigma_Q^2 \cdot \mathbf{G}^{\mathrm{noise}} \cdot (\mathbf{G}^{\mathrm{noise}})^{\mathrm{H}}}_{\mathbf{C}_{\mathrm{n}}}.\end{aligned} \tag{16}$$

Hence, the SINR related to the k^{th} subcarrier is given as

$$\mathrm{SINR}(k) = \frac{[\mathbf{C}_{\mathrm{s}}]_{kk}}{[\mathbf{C}_{\mathrm{i}}]_{kk} + [\mathbf{C}_{\mathrm{n}}]_{kk}}. \tag{17}$$

When QAM is used and error probability is measured in terms of symbol error rate (SER), the achievable data rate for the k^{th} subcarrier is

$$C(k) = \log_2\left(1 + \frac{\mathrm{SINR}(k)}{\Gamma}\right), \tag{18}$$

in which the SNR gap Γ for a target SER is $\Gamma = \gamma_{\mathrm{dm}} - \gamma_{\mathrm{c}} + \Gamma_{\mathrm{m}}$ (in decibels), where γ_{dm} is a design margin, γ_{c} is the coding gain, and

$$\Gamma_{\mathrm{m}} = \frac{1}{3}\left[Q^{-1}\left(\frac{\mathrm{SER}}{4}\right)\right]^2, \tag{19}$$

Authorized licensed use limited to: KU Leuven Libraries. Downloaded on December 17,2020 at 09:02:11 UTC from IEEE Xplore. Restrictions apply.

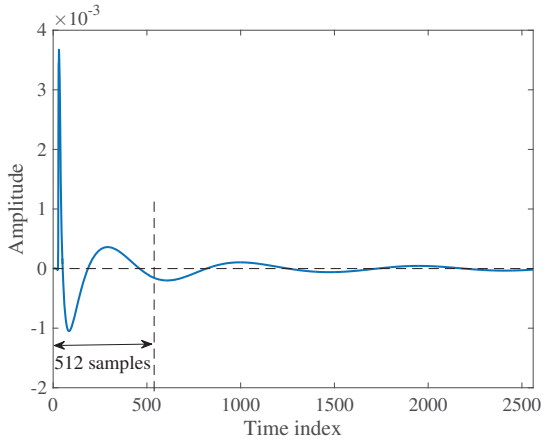


Fig. 2. Response of the CSA loop 4 in series with a high-pass filter.

with $Q(\cdot)$ being the tail distribution function of the normal distribution.

By disregarding the signal correlation among the transceiver sub-channels, the achievable data rate of a suboptimal system can finally be obtained as

$$R = f_s \cdot \frac{N}{N_0} \cdot \sum_{k \in \mathcal{N}} C\,(k), \tag{20}$$

where f_s is the underlying sampling rate.

V. Simulation Results

The SINR calculation is an important task for several applications, including the design of time-domain equalizers (TEQs) and the calculation of achievable data rates. In this context, this section exemplifies two key points: the influence that the limitation of CIR length has on TEQ design, and the differences of calculating the achievable data rate considering the interference limited to two or three blocks (Conventional), versus the one considering the actual dispersion (Actual).

A classic simulation setup, based on the widely used carrier-serving area (CSA) downstream loops [12], [13], is employed to achieve this goal. In the experiments, the CSA loops are in series with a fifth-order Chebyshev Type-I high-pass filter with cut-on frequency at 4.8 kHz, which filters out the telephone voiceband signal [29]. For downstream, the IDFT and DFT have size $N = 512$, which is also the maximum CIR length in the Conventional analysis for obtaining the SINR. However, the convolution of any CSA loop with the high-pass filter has significant samples beyond the 512-sample index. Fig. 2 depicts an example of the convolution of CSA loop 4 with the high-pass filter. The discarded samples beyond the time index 512 correspond to 21.18% of the effective CIR energy. The Actual analysis via the proposed formulation considers all samples in Fig. 2.

To use relatively small CP lengths, one can employ TEQs, which can be designed via classic techniques, such as those proposed in [30] (MSSNR) and [31] (EIGAP). The design

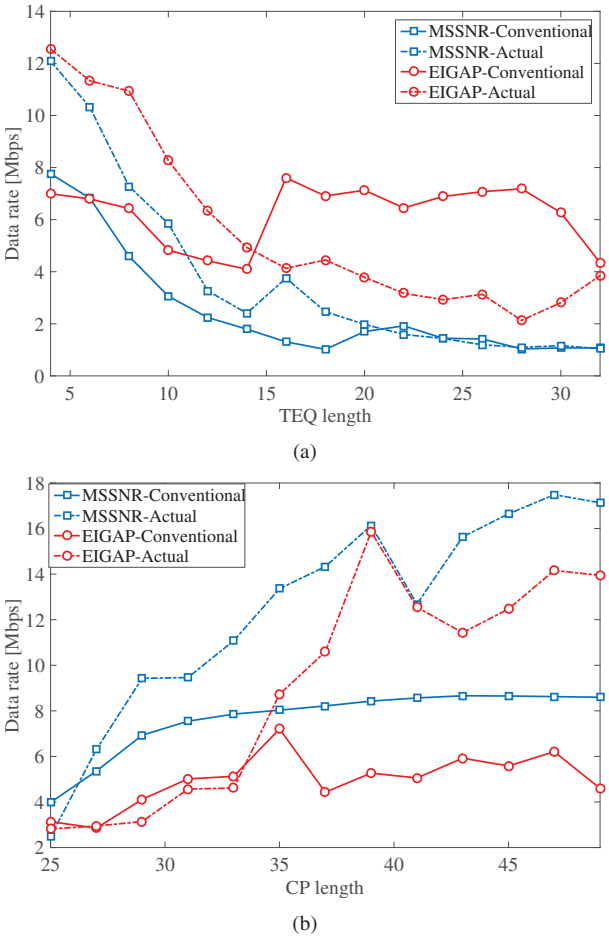


Fig. 3. Achievable data rates as a function of (a) TEQ and (b) CP lengths.

task is conducted considering: the first 512 samples in Fig. 2 (Conventional), or the entire response in Fig. 2 (Actual). Once the TEQs have been designed, the overall impulse responses (OIRs) are obtained by convolving the response in Fig. 2 with the TEQ response. From these OIRs, the achievable data rates are obtained with the interference limited to two or three blocks (Conventional) or to a larger number of blocks (Actual).

Although there are several sources of DSL noise, the achievable data rates are computed by considering only additive white Gaussian noise (AWGN) at -140 dBm/Hz, assuming an input signal power of 23 dBm/Hz [13]. All powers are defined with respect to a 100-Ω resistor. The following parameters were chosen to compute the data rate for each subcarrier k: an SNR gap $\Gamma_{\mathrm{m}} = 9.8$ dB (for a SER $= 10^{-7}$), a noise margin $\gamma_{\mathrm{dm}} = 6$ dB, and a coding gain $\gamma_{\mathrm{c}} = 4.2$ dB. The sampling rate is $f_s = 2.208$ MHz. The active tones are $\{7, 8, \ldots, 256\}$, and the TEQ time-offset has been optimized over the values $\{2, 3, \ldots, 50\}$.

Figs. 3(a) and 3(b) respectively depict the achievable data rates as a function of the TEQ lengths (for a fixed CP length of $\mu = 32$) and as a function of the CP length (for an optimized TEQ length in the range of values from 2 to the CP length of each experiment). The goal of these

Authorized licensed use limited to: KU Leuven Libraries. Downloaded on December 17,2020 at 09:02:11 UTC from IEEE Xplore. Restrictions apply.

simulations is not comparing the design techniques of [30], [31], but showing the differences in the results of the TEQ designs or in the calculation of data rates. As can be seen in Figs. 3(a) and 3(b), the results obtained differ for virtually all the design parameters considered. These differences highlight the importance of using a correct formulation for the above calculations.

VI. Concluding Remarks

This work discussed the impact of highly dispersive channels on OFDM systems when the length of the prefix appended to the transmission block does not meet the requirement to induce uncoupled equalization solution. We derived the SINR and the achievable data rate for suboptimal OFDM systems under arbitrary length finite duration CIR. In addition, and based on the analytical expressions, the work provided some simulations showing the differences between the results obtained by assuming that interference is limited to two or three blocks, versus those considering all interference blocks. In this sense, the theoretical expression derived for the SINR is more suitable to practical scenarios.

References

[1] R. W. Chang, "High-speed multichannel data transmission with bandlimited orthogonal signals," *Bell System Technical Journal*, vol. 45, pp. 1775–1796, Dec. 1966.

[2] S. Weinstein and P. Ebert, "Data transmission by frequency-division multiplexing using the discrete Fourier transform," *IEEE Transactions on Communication Technology*, vol. 19, no. 5, pp. 628–634, Oct. 1971.

[3] S. B. Weinstein, "The history of orthogonal frequency-division multiplexing [History of Communications]," *IEEE Communications Magazine*, vol. 47, no. 11, pp. 26–35, Nov. 2009.

[4] A. Peled and A. Ruiz, "Frequency domain data transmission using reduced computational complexity algorithms," in *Proceedings of the IEEE International Conference on Acoustics, Speech, and Signal Processing (ICASSP)*, vol. 5, Apr. 1980, pp. 964–967.

[5] G. Altin and R. K. Martin, "Bit-error-rate-minimizing channel shortening using post-FEQ diversity combining and a genetic algorithm," *Signal Processing*, vol. 91, no. 4, pp. 1021–1031, Apr. 2011.

[6] F. Zabini, M. Mazzotti, D. Dardari, G. Chiurco, and O. Andrisano, "Performance and stability analysis of echo cancellers based on training sequences," *IEEE Transactions on Broadcasting*, vol. 60, no. 3, pp. 437–451, Sep. 2014.

[7] E. Viterbo and K. Fazel, "How to combat long echoes in OFDM transmission schemes: sub-channel equalization or more powerful channel coding," in *Proceedings of the IEEE Global Telecommunications Conference (GLOBECOM)*, vol. 3, Nov. 1995, pp. 2069–2074.

[8] J. L. Seoane, S. K. Wilson, and S. Gelfand, "Analysis of intertone and interblock interference in OFDM when the length of the cyclic prefix is shorter than the length of the impulse response of the channel," in *Proceedings of the IEEE Global Telecommunications Conference (GLOBECOM)*, vol. 1, Nov. 1997, pp. 32–36.

[9] D. Kim and G. L. Stuber, "Residual ISI cancellation for OFDM with applications to HDTV broadcasting," *IEEE Journal on Selected Areas in Communications*, vol. 16, no. 8, pp. 1590–1599, Oct. 1998.

[10] I. Barhumi, G. Leus, and M. Moonen, "Time-domain and frequency-domain per-tone equalization for OFDM over doubly selective channels," *Signal Processing*, vol. 84, no. 11, pp. 2055–2066, Nov. 2004.

[11] W. Henkel, G. Tauböck, P. Ödling, P. O. Börjesson, and N. Petersson, "The cyclic prefix of OFDM/DMT – An analysis," in *Proceedings of the International Zurich Seminar on Broadband Communications. Access, Transmission, Networking*, 2002, pp. 22–1–22–3.

[12] M. Milosevic, L. F. C. Pessoa, B. L. Evans, and R. Baldick, "DMT bit rate maximization with optimal time domain equalizer filter bank architecture," in *Proceeding of the 36th Asilomar Conference on Signals, Systems and Computers*, vol. 1, Nov. 2002, pp. 377–382.

[13] K. Vanbleu, G. Ysebaert, G. Cuypers, M. Moonen, and K. V. Acker, "Bitrate-maximizing time-domain equalizer design for DMT-based systems," *IEEE Transactions on Communications*, vol. 52, no. 6, pp. 871–876, June 2004.

[14] E. Zöchmann, S. Pratschner, S. Schwarz, and M. Rupp, "Limited feedback in OFDM systems for combating ISI/ICI caused by insufficient cyclic prefix length," in *Proceeding of the 48th Asilomar Conference on Signals, Systems and Computers*, Nov. 2014, pp. 988–992.

[15] T. Pham, T. Le-Ngoc, G. K. Woodward, and P. A. Martin, "Channel estimation and data detection for insufficient cyclic prefix MIMO-OFDM," *IEEE Transactions on Vehicular Technology*, vol. 66, no. 6, pp. 4756–4768, June 2017.

[16] T. Taheri, R. Nilsson, and J. van de Beek, "Asymmetric transmit-windowing for low-latency and robust OFDM," in *Proceedings of the IEEE Global Telecommunications Conference (GLOBECOM)*, Dec. 2016, pp. 1–6.

[17] S. Wang, J. S. Thompson, and P. M. Grant, "Closed-form expressions for ICI/ISI in filtered OFDM systems for asynchronous 5G uplink," *IEEE Transactions on Communications*, vol. 65, no. 11, pp. 4886–4898, Nov. 2017.

[18] B. Lim and Y. C. Ko, "SIR analysis of OFDM and GFDM waveforms with timing offset, CFO, and phase noise," *IEEE Transactions on Wireless Communications*, vol. 16, no. 10, pp. 6979–6990, Oct. 2017.

[19] M. Ouzzif and J. L. Masson, "Statistical analysis of the cyclic prefix impact on indoor PLC capacity," in *Proceeding of the IEEE International Symposium on Power Line Communications and Its Applications*, Mar. 2009, pp. 285–289.

[20] M. Wolkerstorfer, P. Tsiaflakis, M. Moonen, and D. Statovci, "Joint power-loading and cyclic prefix length optimization for OFDM-based power line communication," in *Proceedings of the IEEE International Conference on Acoustics, Speech, and Signal Processing (ICASSP)*, May 2013, pp. 4688–4692.

[21] D. J. F. Barros and J. M. Kahn, "Optimized dispersion compensation using orthogonal frequency-division multiplexing," *Journal of Lightwave Technology*, vol. 26, no. 16, pp. 2889–2898, Aug. 2008.

[22] W. Zhong and Z. Mao, "Efficient time-domain residual ISI cancellation for OFDM-based WLAN systems," *IEEE Transactions on Consumer Electronics*, vol. 52, no. 2, pp. 321–326, May 2006.

[23] J. I. Montojo and L. B. Milstein, "Effects of imperfections on the performance of OFDM systems," *IEEE Transactions on Communications*, vol. 57, no. 7, pp. 2060–2070, July 2009.

[24] T. Pollet, H. Steendam, and M. Moeneclaey, "Performance degradation of multi-carrier systems caused by an insufficient guard interval," in *Proceedings of the International Workshop on Copper Wire Access Systems "Bridging the Last Copper Drop"*, Oct. 1997, pp. 265–270.

[25] S. Das and P. Schniter, "Max-SINR ISI/ICI-shaping multicarrier communication over the doubly dispersive channel," *IEEE Transactions on Signal Processing*, vol. 55, no. 12, pp. 5782–5795, Dec. 2007.

[26] P. Amini and B. Farhang-Boroujeny, "Per-tone equalizer design and analysis of filtered multitone communication systems over time-varying frequency-selective channels," in *Proceeding of the IEEE International Conference on Communications (ICC)*, June 2009, pp. 1–5.

[27] P. Schniter, "Low-complexity equalization of OFDM in doubly selective channels," *IEEE Transactions on Signal Processing*, vol. 52, no. 4, pp. 1002–1011, Apr. 2004.

[28] A. M. Tonello and F. Pecile, "Analytical results about the robustness of FMT modulation with several prototype pulses in time-frequency selective fading channels," *IEEE Transactions on Wireless Communications*, vol. 7, no. 5, pp. 1634–1645, May 2008.

[29] R. K. Martin, K. Vanbleu, M. Ding, G. Ysebaert, M. Milosevic, B. L. Evans, M. Moonen, and C. R. Johnson, "Unification and evaluation of equalization structures and design algorithms for discrete multitone modulation systems," *IEEE Transactions on Signal Processing*, vol. 53, no. 10, pp. 3880–3894, Oct. 2005.

[30] P. J. W. Melsa, R. C. Younce, and C. E. Rohrs, "Impulse response shortening for discrete multitone transceivers," *IEEE Transactions on Communications*, vol. 44, no. 12, pp. 1662–1672, Dec. 1996.

[31] B. Farhang-Boroujeny and M. Ding, "Design methods for time-domain equalizers in DMT transceivers," *IEEE Transactions on Communications*, vol. 49, no. 3, pp. 554–562, Mar. 2001.

Authorized licensed use limited to: KU Leuven Libraries. Downloaded on December 17,2020 at 09:02:11 UTC from IEEE Xplore. Restrictions apply.